Reconstruction of chitosan network order using the meniscus splitting method for design of pH-responsive materials

As natural polymers, polysaccharides are expected to serve as alternative materials toward the development of sustainable society in a broad range of fields such as food packaging, functional foods, drug delivery, cosmetics, and agriculture. The natural polysaccharide chitosan is a product of deacetylated chitin, which is extracted from the exoskeletons of crustaceans and insects and fungal cell walls. Moreover, chitosan is a cationic polymer that has attracted the attention of numerous researchers in various biomedical fields, such as wound healing, hemodialysis membranes, drug and gene delivery systems, and tissue engineering/regeneration [1]. In the chitosan side chain, amino and hydroxyl groups can be employed as cross-linkable groups. Amino groups can be protonated to ammonium groups below pH 6.4, making chitosan a pH-responsive soft material [2].

Recently, several methods, such as pre-stretching and drying, directional freezing, and electrospinning, have been reported for the preparation of polysaccharide-based materials with anisotropic microstructures. Distinct from these methods, we have developed a meniscus splitting method [3,4] for preparing a three-dimensionally ordered polymer membrane by exploiting viscous fingering phenomena. Affected by temperature and humidity, the evaporative interface of the polymer solution/dispersion from a cell induces the orientation of polymeric microfibers along the contact line of the interface by capillary force. During water evaporation, the concentrated polymer at the interface bridges the millimeter-scale gap between the two substrates and forms vertical membranes. The limitation for the bridging distance is essentially ~2 mm, depending on the capillary length.

In particular, chitosan was initially dispersed in an aqueous mixture containing acetic acid and deposited by bridging the gaps and forming a membrane during drying [5]. Polarized light microscopy observation of the membrane revealed that the polarizers and first-order retardation plate (λ = 530 nm) were directionally set, as shown in Fig. 1(a). The membrane formed from two air-liquid phases is shown in blue. This result strongly implies that the membrane has a structure that is oriented parallel to the *Y*-gap axis. However, a part of the membrane appeared somewhat yellow because the sample was slightly curved toward the *X*-axis or tilted to the *Z*-axis rather than parallel to the *Y*-axis. After rewetting the membrane with pure water, and without any additional crosslinker from air, the membrane behaved as a hydrogel with anisotropic swelling (Fig. 1(a)). The swelling ratios, L_{WET}/L_{DRY} in the *X*-, *Y*- and *Z*-directions were 3.1, 1.3, and 1.8, respectively. During drying of the chitosan solution, chemical crosslinkers or crosslinking points were not introduced. Notably, the membrane rapidly and anisotropically swelled in pure water while maintaining its hydrogel shape.

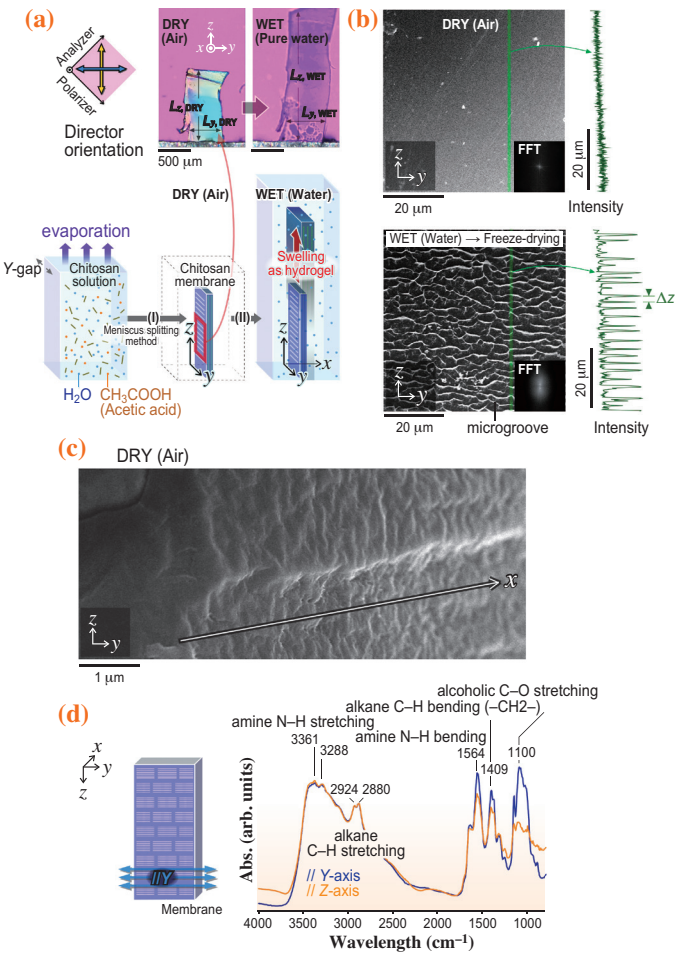

Fig. 1. Chitosan hydrogel swelling anisotropically in pure water and its microstructures. **(a)** Polarized optical microscopy images in air and in pure water. The process of the chitosan solution for the preparation of the DRY membrane and WET hydrogel. **(b)** SEM images of the heat-dried sample prepared using the meniscus splitting method as DRY (air) and freeze-dried sample as WET (water). Inset: Fast Fourier Transform (FFT) analysis of SEM images. The charts indicate surface asperity along the *YZ*-plane of samples by analyzing the intensity of the gray value along the green line in the SEM images. **(c)** SEM images of the heat-dried sample, focusing on the cross-section in the *X*-direction. **(d)** IR spectra of the membrane through polarized light. The blue and orange spectra correspond to measurements with the polarized aligned parallel to the cell gap (*Y*-direction) and cell depth (*Z*-direction), respectively. Room temperature ~25°C; relative humidity ~50%. [5]

To study the microstructures in the DRY/WET states, the samples were observed by scanning electron microscopy (SEM) (Fig. 1(b)). A WET (water) sample was prepared by freeze drying. In contrast to the DRY sample, the WET sample showed striped patterns with microgrooves parallel to the *Y*-axis. This tendency was also confirmed by the results of FFT analysis (Fig. 1(b), inset). Microgrooves were generated during the sample preparation under reduced pressure, enabling mechanical stress. By analyzing the gray values of the green line on the images, the intervals between the microgrooves (Δz) were measured. The average value of Δz was 2.1 μm, and the groove width was <0.3 μm. Such submicron-scale periodicity was also confirmed in the cross-section of the DRY membrane as layers of the *YZ* plane stacked in the *X*-direction (Fig. 1(c)). Considering that the layer-to-layer distance varied in the 0.3–0.5 μm range, the chitosan fibers were easily self-assembled at this submicron-scale, together with the chitin. Furthermore, to elucidate the anisotropy of molecular structures, the dried sample was evaluated by infrared (IR) spectroscopy carried out with polarized light at SPring-8 **BL43IR**. To determine the anisotropy of molecular structures, the dried sample was evaluated by IR spectroscopy carried out with polarized light at 50% relative humidity (Fig. 1(d)). The two significant peaks at approximately 3361 and 3288 cm^{-1} were attributed to the O–H and N–H stretching vibrations of the functional groups, respectively, which are involved in the hydrogen bonding between the chitosan molecules. The peaks at 2880 and 2924 cm^{-1} indicated alkane C–H stretching. The characteristic peaks at 1564, 1409, and 1100 cm^{-1} are attributed to the N–H bending vibration of amine II, alcoholic C–O stretching, and alkane C–H bending, respectively. All bands, except for those at 3288, 3361, and 2880–2924 cm^{-1}, in the direction parallel to the *Y*-axis were stronger than those in the direction parallel to the *Z*-axis. These results can be attributed to the fact that the chitosan nanofibers in the bundled state exposed more side chains parallel to the *Y*-axis.

To understand the three-dimensional anisotropic swelling, the dried membrane was directly immersed into each buffered solution with a wide pH range (2.2–8.0) at ~25°C. Figure 2 shows typical images at a given pH and the pH dependence of the equilibrium swelling ratio. The ratio, *r*, is defined as the ratio of the length in the wet state to that in the dry state, L_{WET}/L_{DRY}. Swelling ratios in each direction are defined as $r_x = L_{WET,\,x}/L_{DRY,\,x}$, for example. In this pH range, r_x was significantly higher than r_y and r_z, and all of the swelling ratios (r_x, r_y, and r_z) in acidic conditions with pH 2.2–4.0 showed higher values. Under acidic conditions, protonation enables water molecules to penetrate the interspaces among the fibers and chains in the fibers. Consequently, certain crosslinking points based on hydrogen bonds can be eliminated. Based on the pH-responsive swelling ratio, this material can be applied in an aqueous environment with a pH signal, with irreversible changes in the pH range of 2–5 and reversible changes in the pH range of 5–8. The decrease in pH from normal cells to cancer cells can be a switching signal not only for mass transporters, such as nanogels and micelles, but also for tissue engineering using stimuli-responsive soft materials.

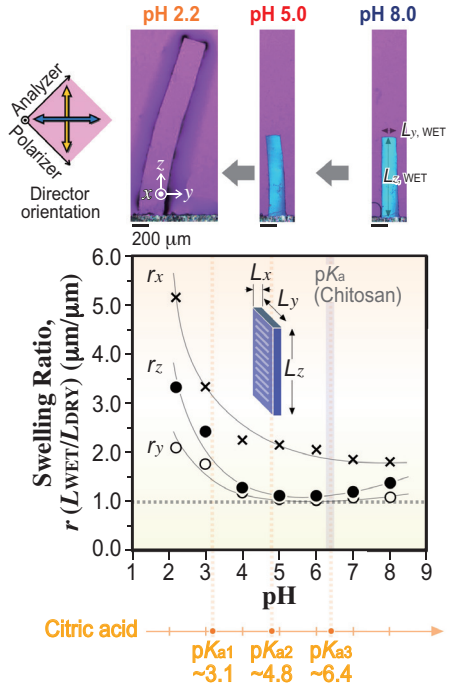

Fig. 2. Chitosan hydrogel with an anisotropic pH response in three dimensions. L_x, L_y, and L_z are the sample lengths in *X*-, *Y*- and *Z*-directions. DRY signifies a condition under air atmosphere at approximately 25°C. The DRY samples were equilibrated in initial pH buffer solutions as the WET state. Buffer solutions consisted of citric acid and disodium. [5]

Thi Kim Loc Nguyen[a], Yuka Ikemoto[b] and Kosuke Okeyoshi[a,*]

[a] Graduate School of Advanced Science and Technology, Japan Advanced Institute of Science and Technology
[b] Japan Synchrotron Radiation Research Institute (JASRI)

*Email: okeyoshi@jaist.ac.jp

References

[1] R. de S. Victor *et al.*: Materials **13** (2020) 4995.
[2] R. Heras-Mozos *et al.*: Carbohyd. Polym. **283** (2022) 119137.
[3] K. Okeyoshi *et al.*: Sci. Rep. **7** (2017) 5615.
[4] K. Okeyoshi: Polym J. **52** (2020) 1185.
[5] *T. K. L. Nguyen, Y. Tonomura, N. Ito, A. Yamaji, G. Matsuba, M. Hara, Y. Ikemoto and K. Okeyoshi: Langmuir* ***40*** *(2024) 11927.*